IOSR Journal of Mathematics (IOSR-JM)
e-ISSN: 2278-5728, p-ISSN: 2319-765X. Volume 12, Issue 5 Ver. IV (Sep. - Oct.2016), PP 71-81
www.iosrjournals.org

Viscous Dissipation Effects on Radiative MHD Boundary Layer Flow of Nano fluid Past a Wedge through Porous Medium with Chemical Reaction

Syam Sundar Majety[1,2], K. Gangadhar[3]
[1](*Department of Nanotechnology, Acharya Nagarjuna University, Andhra Pradesh, India)*
[2](*Research Scholar, Department of Mathematics, Acharya Nagarjuna University, Andhra Pradesh, India)*
[3]*(Department of Mathematics, Acharya Nagarjuna University, Ongole, Andhra Pradesh, India)*

Abstract: *Magnetohydrodynamics (MHD) boundary layer flow past a wedge through porous medium with the influence of thermal radiation, heat source, viscous dissipation and chemical reaction has been analyzed in the present study. The governing nonlinear boundary layer equations for momentum, thermal energy and concentration are transformed to a system of nonlinear ordinary coupled differential equations by using suitable similarity transformation. The transmuted model is shown to be controlled by a number of thermo-physical parameters, viz. the magnetic parameter, heat generation parameter, Permeability parameter, Porosity parameter, Mass and Thermal convective parameters, Prandtl number, Lewis number, Brownian motion parameter, thermophoresis parameter, chemical reaction parameter and pressure gradient parameter. Numerical elucidations are obtained with the legendary Nactsheim-Swigert shooting technique together with Runge–Kutta six order iteration schemes.*

Keywords: *Porous medium; MHD; wedge; radiation; viscous dissipation; chemical reaction*

I. Introduction

It is now well accepted fact that the study of MHD boundary layer flow with thermal radiation and chemical reaction in heat and mass transfer has been encountered in various engineering, technological and manufacturing applications, such as principles of calculation of flow in piping system and oil and gas pipelines, the flow in various pumps, compressors and turbo-machines, problems of heat and mass transfer as found in heat exchangers, boilers and condensers, applications in the field of agricultural engineering, chemical engineering for filtration and purification processes and applications in textile chemical engineering, clothing and thermo physics. At high temperatures, thermal radiation can significantly affect the heat transfer and the temperature distribution in the boundary layer flow of participating fluid. Thermal radiation and chemical reaction effects may play an important role in controlling heat transfer in industry where the quality of the final product depends on heat controlling factors to some extent. Manjula et al. [12] investigated a boundary layer analysis to study the combined effects of thermal radiation and chemical reaction on MHD flow; heat and mass transfer over a stretching surface. Sulochana et al. [23] discussed the influence of radiation and chemical reaction effects on MHD thermosolutal nanofluid flow over a vertical plate in porous medium. Ramachandra et al. [15] reported on the influence of radiation and mass transfer effects on two-dimensional flow past an impulsively started isothermal vertical plate. Heat and mass transfer effects on MHD oscillatory flow in a channel filled with porous medium in presence of radiation and chemical reaction was derived by Ibrahim et al. [7].

Viscous dissipation effects, which are usually characterized by the Eckert number, are important in geophysical flows and also in certain industrial applications such as oil products transportation through ducts. The study of heat transfer in hydrodynamic boundary layer flow over a porous stretching sheet becomes more interesting when internal heat source or absorption occurs. Heat source is important in the context of exothermic or endothermic chemical reactions Srinivasasai et al. [20] analyzed the study of chemical reaction and radiation effects on MHD flow over an exponentially stretching sheet with viscous dissipation and heat source. The effects of heat source on MHD convective flow past a stretching sheet in a micropolar fluid in presence of radiation was studied by Mabood et al. [11]. Suneetha et al. [24] reported radiation and mass transfer effects on MHD free convective dissipative fluid in the presence of heat source/sink. Chamkha [3] investigated thermal radiation and buoyancy effects on hydromagnetic flow over an accelerating permeable surface with heat source or sink. In another article, Shamsuddin et al. [18] described a numerical study on MHD boundary layer flow with viscous dissipation and chemical reaction over a stretching plate in porous medium. Recently, Hadibandhu and Mohapatra [6] studied Dufour and radiation effects on MHD boundary layer flow past a wedge through a porous medium with heat source and chemical reaction. Similarly, Rout et al. [16] investigated the influence of

chemical reaction on MHD heat and mass transfer fluid flow over a moving vertical plate in presence of heat source with convective boundary conditions.

On the other hand, the research of nanofluids has gained huge attention in recent years. Choi [4] was the first to introduce the word nanofluid that represents the fluid in which nano scale particles whose diameter is less than 100 mm. recently; several numerical studies on the modeling of natural convection heat transfer in nanofluids are published. Eshetu and Shankar [5] presented a study on heat and mass transfer through a porous media of MHD flow of nanofluids with thermal radiation, viscous dissipation and chemical reaction effects. Srinivasacharya et al. [21] analyzes the steady laminar MHD flow, heat and mass transfer characteristics in nanofluid over a wedge in the presence of a variable magnetic field. Shakhaoath et al. [17] reported on the MHD radiative boundary layer flow of a nanofluid past a stretching sheet. Chamkha [2] studied radiation effects on mixed convection over a wedge embedded in a porous medium filled with nanofluid. Similarly, Wahiduzzaman et al. [25] investigated viscous dissipation and radiation effects on MHD boundary layer flow of a nanofluid past a stretching sheet. Sugunamma et al. [22] predicted the effects of radiation and magnetic field on the flow and heat transfer of a nanofluid in a rotating frame. Ahmad and Khan [1] employed a quasi linearization technique in studying unsteady heat and mass transfer MHD nanofluid over a stretching sheet with heat source.

Our main objective is to extend the analysis of Shakhaoath et al [19]. This study finds the effect of viscous dissipation and heat source on MHD boundary layer flow past a wedge through porous medium with thermal radiation and chemical reaction. The governing equations are solved numerically using the Nacthsheim-Swigert shooting iteration technique and Runge-Kutta six order iteration scheme and determine the velocity, temperature and concentration profiles.

II. Mathematical Model

We consider the two dimensional MHD laminar boundary layer flow past through a porous medium of an impermeable stretching wedge in presence of thermal radiation, heat generation and chemical reaction and moving with the velocity $u_w(x)$ in a nanofluid, and the free stream velocity is $u_e(x)$, where *x* is the coordinate measured along the surface of the wedge (Khan and Pop [8]. Here $u_w(x)>0$ corresponds to a stretching wedge surface velocity and $u_w(x)<0$ corresponds to a contracting wedge surface velocity, respectively. Instantaneously at time *t>0*, temperature of the plate and species concentration are raised to $T_w\left(>T_\infty\right)$ and $C_w\left(>C_\infty\right)$ respectively, which are thereafter maintained constant, where T_w, C_w are temperature and species concentration at the wall and T_∞, C_∞ are temperature and species concentration far away from the plate respectively. A strong magnetic field $B=\left(0,B_0,0\right)$ is applied in the *y*-direction. Under the above assumptions and usual boundary layer approximation, the MHD mixed convective nanofluid flow governed by following equations (Nield and Kuznetsov [14], Kuznetsov and Nield [9]

$$\frac{\partial u}{\partial x}+\frac{\partial v}{\partial y}=0, \tag{1}$$

$$u\frac{\partial u}{\partial x}+v\frac{\partial v}{\partial y}=u_e\frac{du}{dx}+\upsilon\frac{\partial^2 u}{\partial y^2}+g\beta_T\left(T-T_\infty\right)+g\beta_C\left(C-C_\infty\right)-\frac{\sigma B_0^2}{\rho}u-\frac{\upsilon}{k'\rho}u \tag{2}$$

$$u\frac{\partial T}{\partial x}+v\frac{\partial T}{\partial y}=\alpha\frac{\partial^2 T}{\partial y^2}+\frac{Q}{\rho C_p}\left(T-T_\infty\right)+\frac{16}{3}\frac{\sigma_1 T_\infty^3}{k\rho C_p}\frac{\partial^2 T}{\partial y^2}+\frac{\mu}{\rho C_p}\left(\frac{\partial u}{\partial y}\right)^2+\tau\left\{D_B\left(\frac{\partial T}{\partial y}\frac{\partial C}{\partial y}\right)+\frac{D_T}{T_\infty}\left(\frac{\partial T}{\partial y}\right)^2\right\} \tag{3}$$

$$u\frac{\partial C}{\partial x}+v\frac{\partial C}{\partial y}=D_B\frac{\partial^2 C}{\partial y^2}+\frac{D_T}{T_\infty}\frac{\partial^2 T}{\partial y^2}-k_r\left(C-C_\infty\right) \tag{4}$$

Here in equation (2) the 3rd term on the right hand side is the convection due to thermal expansion and gravitational acceleration, the 4th term on the right hand side is the convection due to mass expansion and gravitational acceleration, the 5th term generated by the magnetic field strength because a strong magnetic field $B=\left(0,B_0,0\right)$ is applied in the y-direction and 6th term represents the porous medium. Again in equation (3) the 2nd term on the right hand side is the effect of heat generation on temperature flow, 3rd term on the right

hand side expressed the radiative heat transfer flow, the second term on the right side is the viscous-dissipation term and the last term indicates the Brownian motion due to nanofluid heat and mass transfer flow.
Also in equation (4) the 2nd term on the right hand side is the thermophoresis diffusion term due to nanofluid flow and the 3rd term is the rate of chemical reaction on the net mass flows.
And the boundary condition for the model is;

$$u = u_w(x) = -\lambda u_e(x),\ v = 0,\ T = T_w,\ C = C_w, \quad \text{at } y = 0$$
$$u = u_e(x),\ T \to T_\infty,\ C \to C_\infty, \quad \text{as } y \to \infty \tag{5}$$

where *u* and *v* are *x* (along the sheet) and *y* (normal to the sheet) components of the velocities respectively, *g* is the acceleration due to gravity, *T* is the fluid temperature, T_∞ is the ambient temperature as *y* tends to infinity, T_w is the temperature at the wedge surface, *C* is the nano particle concentration, C_∞ is the ambient nano particle concentration as *y* tends to infinity, k' is the permeability of porous medium, C_w is the nanoparticle concentration at wedge, C_p is the specific heat capacity, *D* is the coefficient of mass diffusivity, D_B is the Brownian diffusion coefficient, D_T is the thermophoresis diffusion coefficient, α is the thermal diffusivity, β_T is the coefficient of thermal expansion, β_C is the coefficient of mass expansion, σ_1 is the Stefan-Boltzmann constant, *k* is the mean absorption coefficient, σ is the electric conductivity of the fluid, ρ is the density of the fluid, τ is the ratio between the effective heat capacity of the nano particle material and heat capacity of the fluid, λ is the constant moving parameter and k_r is the reaction rate parameter.

In order to conquers a similarity solution to eqs. (1) to (4) with the boundary conditions (5) the following similarity transformations, dimensionless variables are adopted in the rest of the analysis;

$$\eta = y\left(\sqrt{\frac{(1+m)u_e}{2xv}}\right), \qquad \psi = \sqrt{\left(\frac{2u_e xv}{1+m}\right)} f(\eta), \qquad \theta(\eta) = \frac{T - T_\infty}{T_w - T_\infty} \qquad \phi(\eta) = \frac{C - C_\infty}{C_w - C_\infty}$$

$$\text{and } u = \frac{\partial \psi}{\partial y},\ v = -\frac{\partial \psi}{\partial x} \tag{6}$$

For the similarity solution of equation (1) to (4) with considering the value (from the properties of wedge, see Lin and Lin [10]) $u_e(x) = ax^m$, $u_w(x) = cx^m$, where *a*, *c* and *m* $(0 \le m \le 1)$ are positive constant. Therefore, the constant moving parameter λ is defined as $\lambda = c/a$, whereas $\lambda < 0$ relates to a stretching wedge, $\lambda > 0$ relates to a contracting wedge, and $\lambda = 0$ corresponds to a fixed wedge, respectively.

From the above transformations the non-dimensional, nonlinear, coupled ordinary differential equations are obtained as;

$$f'''(\eta) + f(\eta) f''(\eta) + \beta\left(1 - f'(\eta)^2\right) + \lambda_T \theta(\eta) + \lambda_M \phi(\eta) - (M + K) f'(\eta) = 0 \tag{7}$$

$$\left(\frac{1+R}{\Pr}\right)\theta''(\eta) + f(\eta)\theta'(\eta) + N_b \theta'(\eta)\phi'(\eta) + N_t \theta'(\eta)^2 + Q\theta(\eta) + Ecf''(\eta) = 0 \tag{8}$$

$$\phi''(\eta) + \frac{N_t}{N_b}\theta''(\eta) + L_e f(\eta)\theta'(\eta) - \gamma \mathrm{R}_e L_e \phi(\eta) = 0 \tag{9}$$

The transformed boundary conditions are as follows;

$$f = 0, \quad f' = -\lambda, \quad \theta = 1, \quad \phi = 1 \quad \text{at } \eta = 0$$
$$f' = 1,\ \theta = 0, \quad \phi = 0 \quad \text{as } \eta \to \infty \tag{10}$$

where the notation primes denote differentiation with respect to η and the parameters are defined as:

Magnetic field parameter, $M = \frac{2\sigma B_0^2}{\rho(1+m)u_e}$ heat generation parameter, $Q = \frac{2Q_0 x}{\rho C_p (m+1)u_e}$, Eckert number, $Ec = \frac{u_w^2}{C_p(T_w - T_\infty)}$, Lewis number, $L_e = \frac{\upsilon}{D_B}$, Brownian motion parameter, $N_b = \frac{(\rho C_p)_p D_B (C_w - C_\infty)}{\upsilon(\rho C_p)_f}$, Thermophoresis parameter, $N_t = \frac{(\rho C_p)_p D_T (T_w - T_\infty)}{\upsilon T_\infty (\rho C_p)_f}$, Radiation parameter, $R = \frac{16}{3}\frac{\sigma_1 T_\infty^3}{\rho C_p k_1 \nu}$, Chemical reaction parameter, $\gamma = \frac{2k_r\upsilon}{u_2^2(1+m)}$., Pressure gradient parameter, $\beta = \frac{2m}{m+1}$, Grashof number, $G_r = \frac{2g\beta_T (T_w - T_\infty)x^3}{(m+1)\nu^2}$, Modified Grashof number, $G_m = \frac{2g\beta_C (C_w - C_\infty)x^3}{(m+1)\nu^2}$, Thermal convective parameter, $\lambda_T = \frac{G_r}{R_e^2}$, Mass convective parameter, $\lambda_M = \frac{G_m}{R_e^2}$, Permeability parameter $K = \frac{2\upsilon x}{k'p(1+m)u_e}$, Local Reynolds number, $R_e = \frac{xu_e}{\nu}$, Prandtl number, $P_r = \frac{\upsilon}{\alpha}$, Heat generation.

For the type of flow under consideration, the main physical quantities of interest are the skin-friction coefficient $f''(0)$, the local Nusselt number $\theta'(0)$, which represent the wall shear stress and the heat transfer rate at the surface and local Sherwood number $\phi'(0)$, which represent the wall shear stress and the mass transfer rate the surface.

III. Numerical Solution

The dimensionless Eqs. (7) - (9) are coupled nonlinear partial differential equations, which are to be solved by using boundary conditions (10). It is difficult to obtain the analytical solution of this set of equations with prescribed boundary conditions. So, here an attempt has been made to seek approximate solutions to this set of equations. To obtain the numerical solutions of Eqs. (7) - (9) for velocity, temperature and concentration field, along with boundary conditions (10), we have used standard initially value solver the shooting method. For the purpose of this method, the Nactsheim-Swigert shooting iteration technique (Nachtsheim and Swigert [13] together with Runge–Kutta six order iteration scheme is taken and determines the velocity, temperature and concentration as a function of the coordinate η. Philip R. Nachtsheim and Paul Swigert presented a method for the numerical solution of the differential equations of the boundary layer type in 1965. For the purpose of present problem, we applied the Nacthsheim-Swigert iteration technique.

In shooting method, the missing (unspecified) initial condition at the initial point of the interval is assumed and the differential equation is integrated numerically as an initial value problem to the terminal point. The accuracy of the assumed missing initial condition is then checked by comparing the calculated value of the dependent variable at the terminal point with its given value there, if a difference exists, another value of the missing initial condition must be assumed and the process is repeated. This process is continued until the agreement between the calculated and the given condition at the terminal point is within the specified degree of accuracy. For this type of iterative approach, one naturally inquires whether or not there is a systematic way of finding each succeeding (assumed) value of the missing initial condition.

The boundary conditions equation (10) associated with the ordinary nonlinear differential equations of the boundary layer type is of the two-point asymptotic class. Two point boundary conditions have values of the dependent variable specified at two different values of the independent variable. Specification of an asymptotic boundary condition implies the value of velocity approaches to unity and the value of temperature approaches to zero as the outer specified value of the independent variable is approached. The method of numerically integrating two-point asymptotic boundary value problem of the boundary layer type, the initial value method, requires that the problem be recast as an initial value problem. Thus it is necessary to set up as many boundary conditions at the surface as there are at infinity. The governing differential equations are then integrated with

these assumed surface boundary conditions. If the required outer boundary condition is satisfied, a solution has been achieved.

However, this is not generally the case. Hence a method must be devised to logically estimate the new surface boundary conditions for the next trial integration. Asymptotic boundary value problems such as those governing the boundary layer equations are further complicated by the fact that the outer boundary condition is specified at infinity. In the trial integration infinity is numerically approximated by some large value of the independent variable. There is no a priori general method of estimating this value. Selection of too small a maximum value for the independent variable may not allow the solution to asymptotically converge to the required accuracy. Selecting a large value may result in divergence of the trial integration or in slow convergence of surface boundary conditions required satisfying the asymptotic outer boundary condition. Selecting too large a value of the independent variable is expensive in terms of computer time. Nachtsheim-Swigert developed an iteration method, which overcomes these difficulties.

From the process of numerical computation, the skin-friction coefficient, Nusselt number and Sherwood number which are respectively proportional to $f''(0)$, $\theta'(0)$ and $\phi'(0)$ are also sorted out and their numerical values are presented in a tabular form.

IV. Results and Discussion

In order to investigate the physical representation of the problem, the numerical values of velocity (f'), temperature (θ) and concentration (φ) have been computed for resultant principal parameters as the Magnetic parameter *M*, permeability parameter *K*, pressure gradient parameter β, constant moving parameter l, Thermal convective parameter λ_T, Mass convective parameter λ_M, local Reynolds number R_e, Prandtl number *Pr*, Viscous dissipation parameter *Ec*, Heat source parameter *Q*, Lewis number *Le*, Brownian motion parameter N_b, thermophoresis parameter N_t, radiation parameter *R* and chemical reaction parameter γ respectively. In the present study, the following default parameter values are adopted for computations: *M =0.5, K = 0.5,* $\lambda_T = 6.0,\ \lambda_M = 3.0,$ *Q = 0.5, R = 1.0, Pr = 0.71,* $N_b = 0.3$, $N_t = 0.3$, $\gamma = 1.0$, *Le = 3.0,* $R_e = 1.0$, $\beta = 1.0$, *Ec = 0.1.* All graphs therefore correspond to these values unless specifically indicated appropriately.

In order to test the accuracy of the present method, our results are compared with those of White [26], Yih [28], Yacob et al. [27], Khan and Pop [8] and Shakhaoath Khan et al. [19] (for reduced cases) and found that there is an excellent agreement, as shown in Table1.

Figure 2 reveals the effects of thermal convective parameter λ_T on the velocity profile. It is observed that increases in the thermal convective parameter strongly accelerate the flow thereby increasing the momentum boundary layer. Figure 3 represents the velocity profile for different values of mass convective parameter λ_M. An increase in mass convective (species buoyancy) parameter, as shown in Fig. 3, generally heats the momentum boundary layer and causes the velocity fluid to increase in the nanofluid. Figure 4 depicts the influence of magnetic field parameter *M* on velocity profile. It is evident that the velocity profile decreases with increase in magnetic field strength. The effect of magnetic field on an electrically conducting fluid give rise to a resistive type force called Lorentz force. This force has tendency to slow down the motion of the fluid in the boundary layer thickness. Figure 5 shows the effect of the permeability parameter *K* on velocity profile with different values of constant moving parameter l. It is clear that the increase in *K* leads to decrease in the velocity of the nanofluid on the porous wall and so enhance the momentum boundary layer thickness. Figure 6 exhibits the velocity profile for different values of pressure gradient parameter β. An increase in the pressure gradient parameter is observed to strongly retard the flow. Therefore the velocity decreases within the boundary layer as pressure gradient increase.

In figures 7 and 8, velocity and temperature profiles are plotted for different values of Heat source parameter *Q*. From the graphs it is clear that there is an increase in both the velocity and temperature profiles of the fluid with an increase in heat source parameter. This is because when heat is absorbed, the buoyancy forces and the thermal diffusivity of the fluid increase, which accelerate the flow rate and thereby give rise to an increase in the velocity and temperature profiles. Figure 9 and 10 illustrates the effect of radiation parameter *R* on the velocity and temperature profiles of the flow. It is observed a hike in the velocity and temperature profiles for higher values of the radiation parameter. Generally, an increase in the radiation parameter releases the heat energy to the flow. This causes to develop the momentum and thermal boundary layer thickness. The influence of viscous dissipation parameter *Ec* on the velocity, temperature and concentration profiles is reported in figure 11, 12 and 13 respectively. The Eckert number embodies the conversion of kinetic energy into internal energy by work done against the viscous fluid stress. It is observed that greater viscous dissipative heat causes an increase in the velocity and temperature profiles across the boundary layer as shown in figure 11 and 12, while reverse trend is observed in figure 13 whereby the concentration profile gradually decrease with increase in viscous dissipation parameter.

Figure 14 and 15 displays the typical temperature and concentration profiles for different values of the thermophoresis parameter N_t. The thermophoresis force generated by the temperature gradient creates a fast flow from the surface. In this way more fluid is heated away from the surface and consequently, as N_t increases, both the temperature and concentration profiles increases in the boundary layer. Figures 16 and 17 illustrate the effects of an increase in the Brownian motion parameter N_b on the temperature and concentration. It is observed that as the Brownian motion parameter increases, the temperature profile increase, especially in the region close to the wedge surface. However, it is remarked that there is a sharp fall in the concentration profile near the plate. Clearly, increases in N_b decrease the concentration profile near the plate. Figure 18 reveals the influence of different values of Prandtl number *Pr* on the temperature profile. It can be seen that the temperature gradually decreases with an increase in *Pr*. This is because, as Pr increases, the thermal diffusivity of the fluid reduce and causes weak penetration of heat inside the fluid and consequently, reduces the temperature profile of the fluid.

Figures 19 and 20 reports the concentration profile for different values of Lewis number *Le* and local Reynolds number R_e. It is clearly observed that the concentration profile and its boundary layer thickness decrease considerably as the Lewis number increase. Also, with the increase in local Reynolds number we noticed similar type of result as we observed in figure 19. Generally, increasing in *Le* and R_e reduces the concentration boundary layer. This results in the enhancement of heat and mass transfer. Figure 21 illustrates the concentration profile for different values of chemical reaction parameter γ. It is evident that the increase in chemical reaction parameter significantly alters the concentration boundary layer thickness. This causes the concentration buoyancy effect to decrease yielding a reduction in the concentration profile.

Table 2 displays the effects of non-dimensional governing parameters on the skin friction coefficient, Nusselt and Sherwood numbers respectively. It is observed that with decrease in thermal convective parameter λ_T and mass convective parameter λ_M, we noticed depreciation in skin friction, Nusselt number and Sherwood number. But we observed reverse results to above with the increase in magnetic field parameter *M* and permeability parameter *K*. A decrease in pressure gradient parameter β enhances the

Sherwood number. But quite opposite is seen as both the skin friction and Nusselt number decreased as the pressure gradient parameter β decreased. In Table 3 it is seen that a decrease in *R*, N_b, N_t and *Ec* enhances the skin friction and Sherwood number. A reverse trend is seen in the case of Nusselt number. It is also observed from the same Table that an increase in *Pr* and *Q* causes an increase in skin friction and Sherwood number throughout the momentum and concentration boundary layer. In Table 4 it is observed that the *Le*, γ, R_e and l have no effect on the Sherwood number, whereas the skin friction and Nusselt number increases throughout the momentum and thermal boundary layer due to the enhancement of the non-dimensional governing parameters.

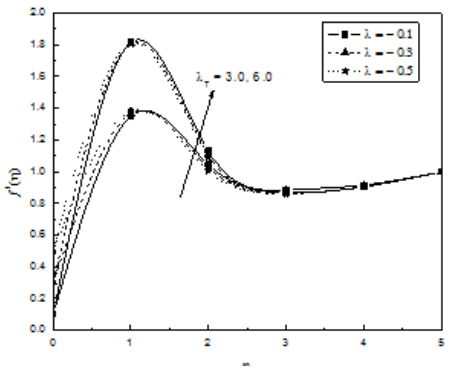

Figure 2 Velocity profile for different values of λ_T

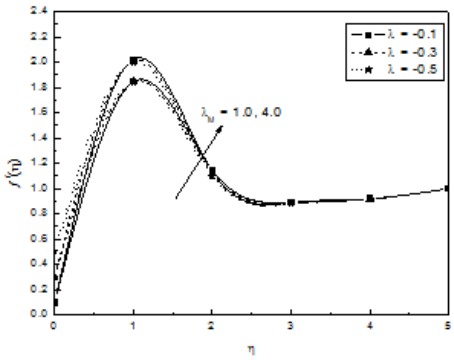

Figure 3 Velocity profile for different values of λ_M

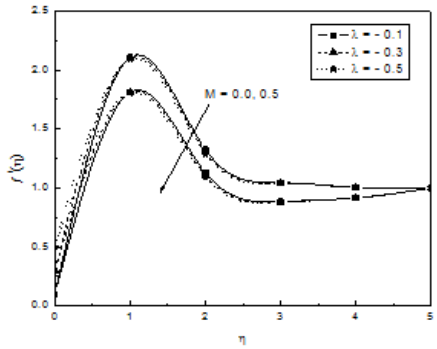

Figure 4 Velocity profile for different values of *M*

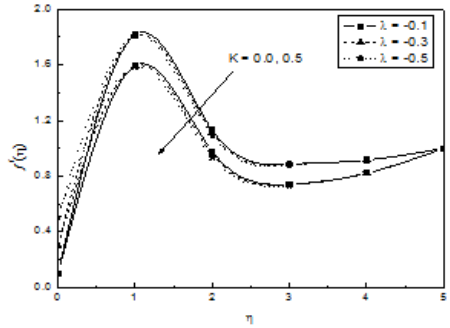

Figure 5 Velocity profile for different values of *K*

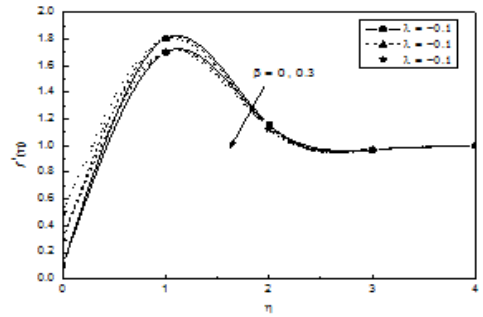

Figure 6 Velocity profile for different values of β

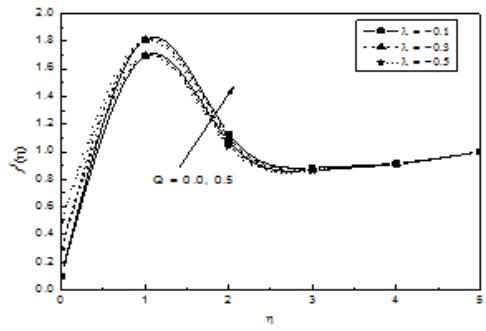

Figure 7 Velocity profile for different values of *Q*

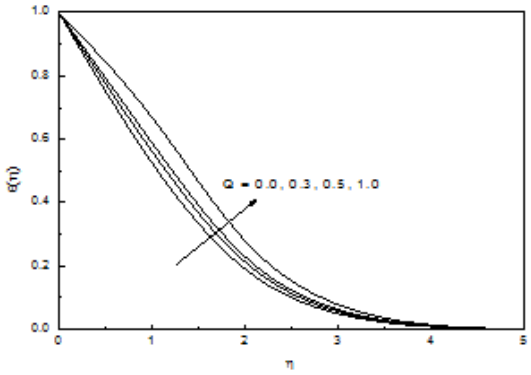

Figure 8 Temperature profile for different values of *Q*

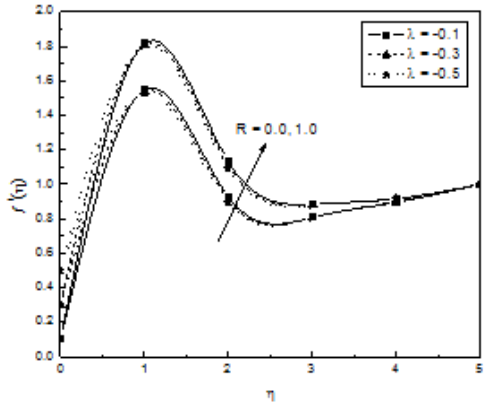

Figure 9 Velocity profile for different values of *R*

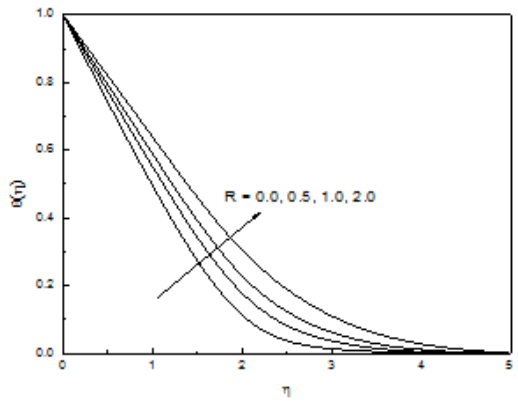

Figure 10 Temperature profile for different values of *R*

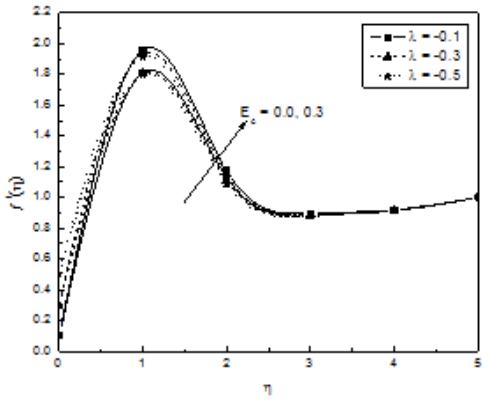

Figure 11 Velocity profile for different values of E_c

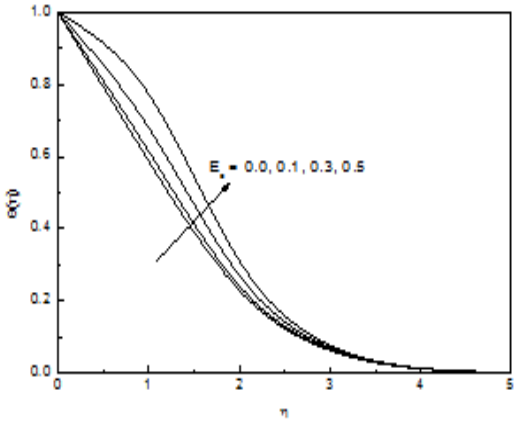

Figure 12 Temperature profile for different values of E_c

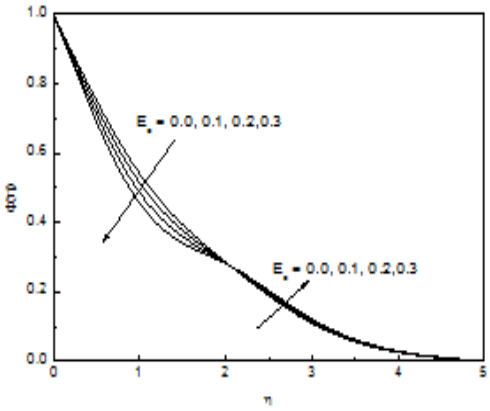

Figure 13 Concentration profile for different values of E_c

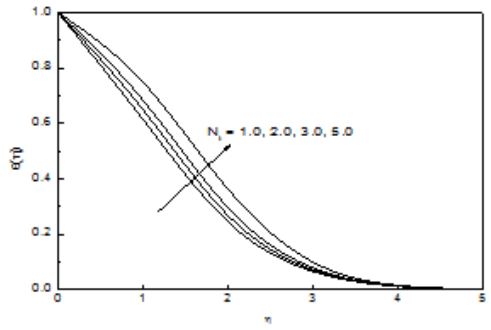

Figure 14 Temperature profile for different values of N_t

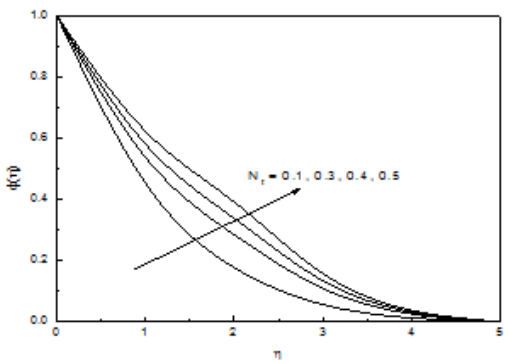

Figure 15 Concentration profile for different values of N_t

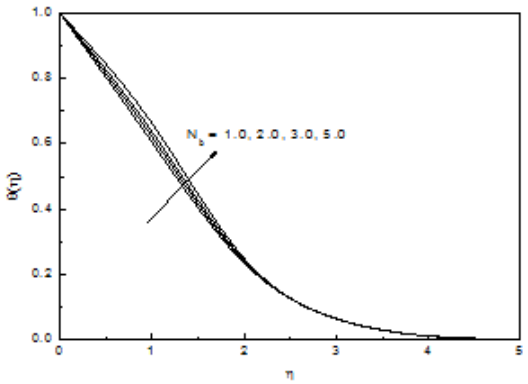

Figure 16 Temperature profile for different values of N_b

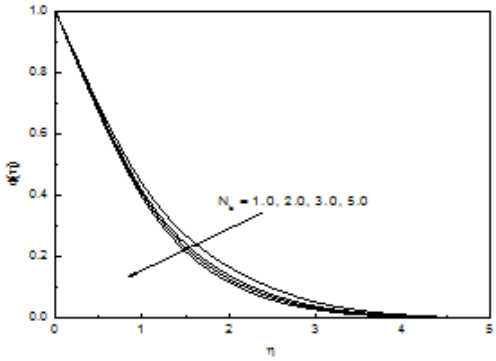

Figure 17 Concentration profile for different values of N_b

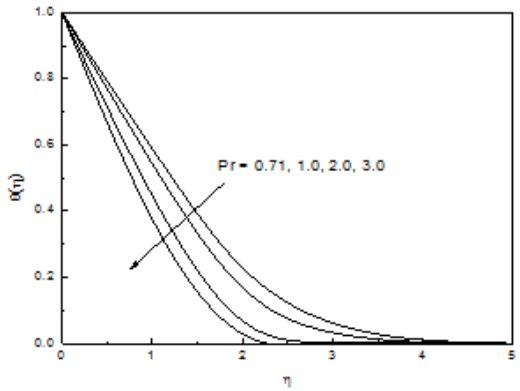

Figure 18 Temperature profile for different values of Pr

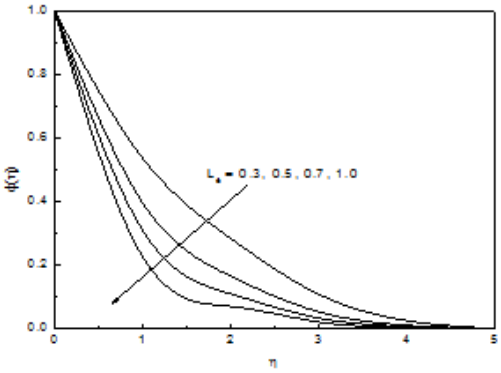

Figure 19 Concentration profile for different values of L_e

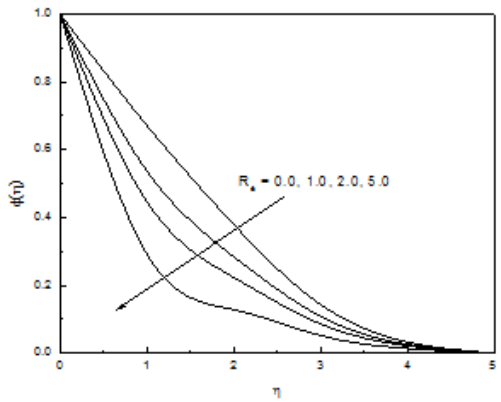

Figure 20 Concentration profile for different values of R_e

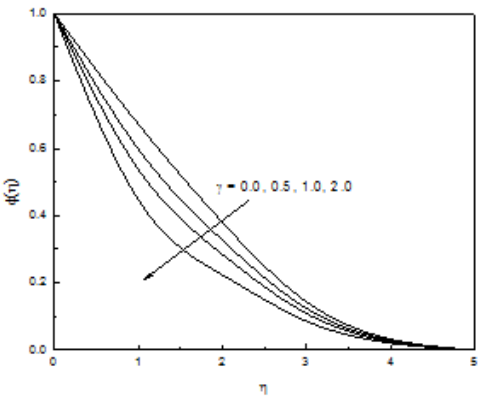

Figure 21 Concentration profile for different values of γ

Table 1: Comparison of the values of skin friction coefficient $f''(0)$ for several values of *m* when

$$\lambda = \lambda_T = \lambda_M = M = K = R = Q = \gamma = Ec = 0$$

m	White [24]	Yih [25]	Yacob et al. [26]	Khan and Pop [19]	Shakhaoath Khan [18]	Present
0	0.4696	0.4696	0.4696	0.4696	0.4699	0.4698
1/11	0.6550	0.6550	0.6550	0.6550	0.6574	0.6571
1/5	0.8021	0.8021	0.8021	0.8021	0.8045	0.8032
1/3	0.9277	0.9276	0.9276	0.9277	0.9298	0.9286
½	1.0389	-	-	1.0389	1.0394	1.0389
1	1.2326	-	1.2326	1.2326	1.2358	1.2351

Table 2: Effects of thermal convective parameter λ_T, mass convective parameter λ_M, magnetic field parameter *M*, pressure gradient parameter β for *Pr = 0.71,R = 1.0, N_b = 0.3, N_t = 0.3, Ec = 0.1, Q = 0.5, Le = 3.0, γ = 1.0, R_e = 2.0,* and λ *= 0.1.*

λ_T	λ_M	M	β	K	$f''(0)$	$\theta'(0)$	$\phi'(0)$
6	3	0.5	1.0	0.5	4.56941	0.513283	3.57019
2					2.65015	0.469789	3.44698
4					3.56818	0.488078	3.51112
	1				2.23979	0.502086	3.55975
	2				3.05941	0.504983	3.57019
		1.0			4.99075	0.518893	3.61426
		2.0			4.08759	0.492893	3.53842
			0.1		4.46762	0.504018	3.57050
			0.3		4.47784	0.504061	3.57089
				1.0	4.27552	0.235651	2.62806
				2.0	3.79728	0.184365	2.58912

Table 3: Effects of Prandtl number *Pr*, radiation parameter *R*, Brownian motion parameter N_b, thermopheresis parameter N_t, Eckert number *Ec*, and heat generation *Q* for λ_T *=6.0,* λ_M *= 3.0, M = 0.5, K = 0.5,* β *= 1.0, Le = 3.0,* γ *= 1.0,* R_e *= 2.0,* and λ *= 0.1.*

Pr	*R*	N_b	N_t	*Ec*	*Q*	$f''(0)$	$\theta'(0)$	$\phi'(0)$
0.71	1.0	0.3	0.3	0.1	0.5	4.56941	0.51328	3.57019
1.0						4.66644	0.23234	3.70688
2.0						4.67483	0.31456	3.64451
	0.1					4.65941	0.44234	3.55019
	0.5					4.65624	0.40987	3.58195
		0.1				4.66040	0.46784	3.54367
		0.5				4.64124	0.42356	3.62460
			0.1			4.65805	0.45678	3.69942
			0.5			4.64372	0.43256	3.62019
				0.01		4.66191	0.42567	3.57269
				0.05		4.65611	0.39765	3.59248
					1.0	4.84568	0.46758	3.81894
					2.0	4.57589	0.24567	3.95479

Table 4: Effects of Lewis number Le, chemical reaction parameter γ , Reynolds number R_e , and constant moving parameter λ for λ_T *=6.0,* λ_M *= 3.0, M = 0.5, K = 0.5,* β *= 1.0, Pr = 0.71,R = 1.0, N_b = 0.3, N_t = 0.3, Ec = 0.1,* and *Q = 0.5.*

Le	γ	R_e	λ	$f''(0)$	$\theta'(0)$	$\phi'(0)$
5.0	1.0	1.0	0.5	4.56941	0.513283	3.57019
1.0				4.83817	0.538918	1.35052
3.0				4.71178	0.533305	2.12947
	0.1			4.73435	0.533455	1.67669
	0.5			4.69126	0.532337	2.15609
		0.5		4.74517	0.501842	3.08868
		0.7		4.71556	0.501025	3.29744
			0.1	4.60903	0.526518	3.5105
			0.3	4.90967	0.517721	3.43192

V. Conclusions

This paper presents the problem radiative MHD dissipative heat generating and chemical reacting nanofluid flow past a wedge through a porous medium. The governing nonlinear partial differential equations were transformed into ordinary differential equations using the similarity approach and solved numerically using Nactsheim-Swigert shooting technique together with Runge–Kutta six order iteration schemes. From the above discussions we conclude the following

(i) Viscous dissipation produces heat due to drag between the fluid particles, which causes an increase in fluid temperature.
(ii) Presence of magnetic field produces a Lorentz force which usually resists the momentum field.
(iii) Presence of porous parameter is beneficial to generate heat in the system.
(iv) High Prandtl number causes low thermal diffusivity.
(v) The skin-friction at the surface increases with increasing buoyancy parameters.
(vi) The heat transfer rate at the boundary surface decreases with increasing thermal radiation, heat source and Eckert number.
(vii) The mass transfer rate at the boundary surface increases with increasing with Lewis number and chemical reaction parameter.

Reference

[1] Ahmad, R., and W.A. Khan (2015). Unsteady heat and mass transfer magnetohydrodynamic (MHD) nanofluid flow over a stretching sheet with heat source-sink using quasi linearization technique, *Canadian J. of physics, 93(12), 1477-1485.*

[2] Chamkha, A.J., S. Abbasbandy, A. M. Rashad, and K. Vajravelu (2012). Radiation effects on mixed convection over a wedge embedded in a porous medium filled with a nanofluid, *Trans. Porous Med., 91, 261-279.*

[3] Chamkha, A.J. (2000). Thermal radiation and buoyancy effects on hydromagnetic flow over an accelerating permeable surface with heat source or sink, *Int. J. Heat Mass Transfer*, 38, 1699-1712.

[4] Choi S.U.S. (1995). Enhancing thermal conductivity of fluids with nano particles, *Devels Appls Non Newtonian Flows*, 66, 99-105.

[5] Eshetu, H. and B. Shankar (2014). Heat and mass transfer through a porous media of MHD flow of nanofluids with thermal radiation, viscous dissipation and chemical reaction effects, *American Chemical Science, Journal*, 4(6), 824-846.

[6] Hadibandhu, P. and R. Mohapatra (2015). Dufour and radiation effects on MHD boundary layer flow past a wedge through a porous medium with heat source and chemical reaction, *J. of Advances in Mathematics*, 11(4), 5094-5107.

[7] Ibrahim S.M., K. Gangadhar, and N Bhaskar Reddy (2015). Radiation and mass transfer effects onMHD oscillatory flow in a channel filled with porous medium in presence of chemical reaction, *J. Applied Fluid Mechanics*, 8(3), 529-537.

[8] Khan, W.A., and I. Pop (2013). Boundary layer flow past a wedge moving in a nanofluid, *Mathematical Problems in Engineering*. Vol. 2013, Article ID 637285, pages 7.

[9] Kuznetsov, A.V., and D. A. Nield (2010). Natural convective boundary-layer flow of a nanofluid past a vertical plate. *Int. J. of Thermal Sci.* 49, 243–247.

[10] Lin, H.T., and L. K Lin (1987). Similarity solutions for laminar forced convection heat transfer from wedges to fluids of any Prandtl number. *Int. J. Heat Mass Transfer*, 30, 1111–1118.

[11] Mabood, F., S.M. Ibrahim, M.M. Rashidi, M.S. Shadloo, and Giulio Lorenzini (2016). Non-uniform heat source/sink and Soret effects on MHD non-Darcian convective flow past a stretching sheet in a micropolar fluid with radiation, *Int. J. Heat and Mass Transfer*, 93, 674-682.

[12] Manjula, J., P. Polarapu, G. M. Reddy, and M. Venakateswarlu (2015). Influence of thermal radiation and chemical reaction on MHD flow, heat and mass transfer over a stretching surface. *Procedia Engineering*, 127, 1315-1322.

[13] Nachtsheim, P.R., and P. Swiger (1965). Satisfaction of the asymptotic boundary conditions in numerical solution of the system of non-linear equations of boundary layer type. NASA, TND-3004, Washington DC.

[14] Nield, A., and A. V. Kuznetsov (2009). The Cheng–Minkowycz problem for natural convective boundary-layer flow in a porous medium saturated by a nanofluid. *Int. J. Heat and Mass Transfer*, 52, 5792–5795.

[15] Ramachandra, P., N. R. Bhaskar, and R. Muthucumaraswamy (2007). Radiation and mass transfer effects on two-dimensional flow past an impulsively started isothermal vertical plate. *Int. J. of Thermal Sciences*, 46(12), 1251-1258.

[16] Rout, B.R., S. K. Parida, and S. Panda (2013). MHD heat and mass transfer of chemical reaction fluid flow over a moving vertical plate in presence of heat source with convective boundary conditions, *Int. J. of Chemical Engineering*, Volume 2013, Article 296834, 1-10.

[17] Shakhaoath, K., Md. A. Alam, and M. Ferdows (2011). MHD radiative boundary layer flow of a nanofluid past a stretching sheet, *Proceedings of the Int. Conference on Mechanical Engineering and Renewable Energy*, 22-24 December 2011, Chittago, Bangladesh, 1-6.

[18] Shamsuddin, MD., P. M. Gayathri, and V. Kumar (2013). MHD boundary layer flow with viscous dissipation and chemical reaction over the stretching porous plate in porous medium. *Int. J. of Mathematical Archive*, 4(2), 328-335.

[19] Shakhaoath Khan Md., Md. Ifsana Karim, Md. Sirajul Islam, and M. Wahiduzzaman (2014). MHD boundary layer radiative, heat generating and chemical reacting flow past a wedge moving in a nanofluid, *Nano Convergence*, 1(20), 1-13.

[20] Srinivasasai P., K. R. Krishna, N. Puppala, and K. J. Remmy (2015). Effects on MHD flow over an exponentially stretching sheet with viscous dissipation and heat generation, *Int. J. of Computer Applications Research*, 5(3), 35-48.

[21] Srinivasacharya, D., U. Mendu, and K. Venumadhav (2015). MHD boundary layer flow of a nanofluid past a wedge, *Procedia Engineering*, 127, 1064-1070.

[22] Sugunamma V., J. V. Ramana Reddy, C. S. K. Raju, M. Jaychandra Babu, and N. Sandeep (2014), Effects of radiation and magnetic field on the flow and heat transfer of a nanofluid in a rotating frame, *Industrial Engineering Letters*, 4(11), 8-20.

[23] Sulochana, C., M. K. Kishor Kumar, and N. Sandeep (2015). Radiation and chemical reaction effects on MHD thermosolutal nanofluid flow over a vertical plate in porous medium. *Chemical and Porous Engineering Research*, 34, 28-37.

[24] Suneetha, S., N. R. Bhaskar, and V. R. Prasad (2011). Radiation and mass transfer effects on MHD free convective dissipative fluid in the presence of heat source/sink, *J. of Applied Fluid Mechanics*, 4(1), 107-113.

[25] Wahiduzzaman, M., Md. Shakhaoath Khan, P. Biswas, Ifsana Karim, and M. S. Uddin (2015). Viscous dissipation and radiation effects on MHD boundary layer flow of a nanofluid past a rotating stretching sheet, *Applied Mathematics*, 6, 547-567.

[26] White F.M. (1991). Viscous Fluid Flow, 2nd edn. (McGraw-Hill, New York, NY, USA.
[27] Yacob N.A., A. Ishak, and I. Pop, (2011). Falkner-Skan problem for a static or moving wedge in nanofluids. *Int. J. Therm. Sci*. 50, 21-28.
[28] Yih, K.A. (1998). Uniform suction/blowing effect on forced convection about a wedge: uniform heat flux. *Acta. Mech*. 128, 173–181.